

THE REGISTRATION OF 3-D MODELS AND A 2-D IMAGE USING POINT AND LINE FEATURES

T. Teo^{a,*}, L. Chen^b

^a Dept. of Civil Engineering, National Chiao Tung University, Hsinchu, Taiwan 30010 - tateo@mail.nctu.edu.tw

^b Center for Space and Remote Sensing Research, National Central University, Taoyuan, Taiwan 32001 - lcchen@csrsr.ncu.edu.tw

KEY WORDS: Image, Three-dimensional, Building, Registration, Orientation

ABSTRACT:

Space registration of 2-D images and 3-D models is an important task for geoinformation applications. Space registration connects the spatial relationship between the image space and object space. It can be implemented by using different control entities like control points, control lines, control surfaces, etc. 3-D models provide both point and line features. Hence, we establish a procedure to determine the image orientation by integrating these features. The objective of this investigation is to combine the point and linear features in space registration. The proposed scheme utilizes collinearity equations in determining the orientation. In this investigation, we compare three kinds of collinearity equations. The first one is a point-based formulation. The second one is line-based equations. The third one is a collinearity model that combines the point and line features. The test data include a simulation data, an aerial image and a close-range image. The experimental results indicate that the proposed scheme is flexible and reliable.

1. INTRODUCTION

A crucial aspect of integrating different geoinformation data is to establish a common reference frame (Zitova and Flusser, 2003). Registration of image and vector data is an important task for various applications, such as cartography, texture mapping, GIS technology, and others. Space registration establishes the spatial relationship between the image space and object space. It can be implemented by using different control entities like points, lines, surfaces, etc. The objective of this investigation is to combine the point and linear features in space registration.

The major work of space registration is to determine the exterior orientation parameters of image data (also called space resection or triangulation). There are three kinds of equations in determining the exterior orientations, i.e., collinearity, coplanarity and coangularity equations (Grussenmeyer and Al Khalil, 2002). The collinearity equations are well-known for orientation determination in photogrammetry field. These equations describe the collinearity geometry of perspective center, image point and object point. They use the intersection of linear-rays to determine the exterior orientations. On the other hand, the coplanarity equations describe the coplanarity geometry of a perspective center, a line in the image space and respective lines in the object space. It uses the intersection of planes to determine the exterior orientations. For coangularity equations, they indicate the coangularity condition among the angles of a perspective center and two object points and the respective angles in a camera frame.

The control entities are used to solve the equations in the orientation modeling. The entities include control points (Wolf and Dewitt, 2000), control lines (Akav et al., 2004; Habib et al., 2005; Jung and Boldo, 2004), control surfaces (Jaw, 2000), control patches (Jaw and Wu, 2006), etc. The control points represent a set of 2-D point features in the image space and 3-D

point features in the object space. The point feature is easy to implement when comparing to others. The control line is a set of 2-D line features in the image space and 3-D line features in the object space. This kind of line features mainly occur in man-made objects like buildings. The control surface describes a set of 2-D point features in the image space and respective 3-D surface models. The control patch includes an image chip database which is used to define the location of the control points. The control patch usually uses image chip database to improve the automation of the point measurement.

The point-based triangulation is widely used in photogrammetric softwares as the control point is the basic control feature. It can be extended to other entities. In some typical scenarios, the linear feature can be measured more flexibly than point feature. Hence, the linear features are often selected in triangulation besides the point features. The vector data provide both control point and control line features. Several investigations have been reported on point-based or linear-based space resection (Karjalainen et al., 2006) from vector data. However, there is a lack of investigation to combine the point and linear features simultaneously on space resection.

In this investigation, we establish a procedure of image orientation determination by integrating point and linear features. The proposed scheme utilizes collinearity equations in the orientation determination. In this paper, we compare three kinds of collinearity equations. The first one is a point-based formulation. The second one is line-based equations. The third one is a joint equation which combines the point and linear features. The test data include a simulation data, an aerial image and a close-range image.

* Corresponding author.

2. METHODOLOGIES

Space registration utilizes space resection to obtain the exterior orientation parameters of image. We introduce three different models in this paper, i.e., point-based space resection, line-based space resection and joint model.

2.1 Point-based Space Resection

The point-based triangulation employs the collinearity equations to solve the exterior parameters. The collinearity equations define the condition of a perspective center, a point in image space and its corresponding object points that are on a straight line. Collinearity equations are shown in Equation 1. Figure 1 illustrates the collinearity condition. As the equations are non-linear with respect to the parameter, we need to linearize the equations and solve the parameters iteratively. The vector, matrix and the elements are shown in Equations 2 and 3. A more detailed description of the procedure can be found in (Wolf and Dewitt, 2000).

$$\begin{aligned} x &= x_0 - f \frac{m_{11}(X - X^c) + m_{12}(Y - Y^c) + m_{13}(Z - Z^c)}{m_{31}(X - X^c) + m_{32}(Y - Y^c) + m_{33}(Z - Z^c)} \\ y &= y_0 - f \frac{m_{21}(X - X^c) + m_{22}(Y - Y^c) + m_{23}(Z - Z^c)}{m_{31}(X - X^c) + m_{32}(Y - Y^c) + m_{33}(Z - Z^c)} \end{aligned} \quad (1)$$

In Equation 1, (x, y) are the image coordinates; (x_0, y_0) are the principal points; (X, Y, Z) are the object coordinates; (X^c, Y^c, Z^c) are the coordinates of perspective center; $(m_{11} \sim m_{33})$ are the elements of rotation matrix from rotation angles (ω, ϕ, κ) ; f is the focal length.

$$V_p = B_p \Delta_p - L_p \quad (2)$$

In Equation 2, V_p is the vector of residual errors; B_p is the matrix of the coefficients of unknowns; Δ_p is the vector of unknown corrections of exterior parameters; L_p is the vector of constant terms. In Equation 3, F and G are the observation functions from collinearity equations.

$$\begin{bmatrix} V_{x1} \\ V_{y1} \\ \vdots \\ V_{xn} \\ V_{yn} \end{bmatrix} = \begin{bmatrix} \frac{\partial F_1}{\partial X^c} & \frac{\partial F_1}{\partial Y^c} & \frac{\partial F_1}{\partial Z^c} & \frac{\partial F_1}{\partial \omega} & \frac{\partial F_1}{\partial \phi} & \frac{\partial F_1}{\partial \kappa} \\ \frac{\partial G_1}{\partial X^c} & \frac{\partial G_1}{\partial Y^c} & \frac{\partial G_1}{\partial Z^c} & \frac{\partial G_1}{\partial \omega} & \frac{\partial G_1}{\partial \phi} & \frac{\partial G_1}{\partial \kappa} \\ \vdots & \vdots & \vdots & \vdots & \vdots & \vdots \\ \frac{\partial F_n}{\partial X^c} & \frac{\partial F_n}{\partial Y^c} & \frac{\partial F_n}{\partial Z^c} & \frac{\partial F_n}{\partial \omega} & \frac{\partial F_n}{\partial \phi} & \frac{\partial F_n}{\partial \kappa} \\ \frac{\partial G_n}{\partial X^c} & \frac{\partial G_n}{\partial Y^c} & \frac{\partial G_n}{\partial Z^c} & \frac{\partial G_n}{\partial \omega} & \frac{\partial G_n}{\partial \phi} & \frac{\partial G_n}{\partial \kappa} \end{bmatrix} \begin{bmatrix} \Delta X^c \\ \Delta Y^c \\ \Delta Z^c \\ \Delta \omega \\ \Delta \phi \\ \Delta \kappa \end{bmatrix} - \begin{bmatrix} F_1 \\ G_1 \\ \vdots \\ F_n \\ G_n \end{bmatrix} \quad (3)$$

2.2 Line-based Space Resection

Line-based space resection applies the linear features as the control features. The linear features can be a straight line or a high-order line (Habib et al., 2003a). The straight lines are mostly selected in line-based space resection. The mathematic model of space resection includes collinearity and coplanarity conditions. Since the collinearity condition is geometrically stronger than the coplanarity one (Schenk, 2004), we select the collinearity approach in this study. Figure 2 illustrates space resection using linear features.

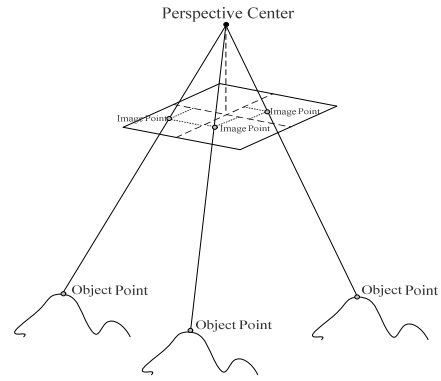


Figure 1. Illustration of point-based triangulation.

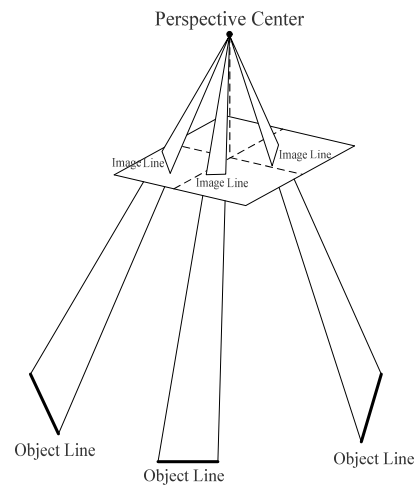


Figure 2. Illustration of line-based triangulation.

First, we need to establish a mathematic model for the line segment. The easiest way to represent a line segment is to use two end points. We can calculate the line parameter from these two end points. The line parameters include the starting point and direction vector. The mathematic model of a line can be formulated as Equation 4. The parameters are not independent and they will cause the ill-condition in solving the exterior orientations. In order to solve the ill-posed problem, we compute the intersection point of the line and plane of $Z=0$ first. Then, we select the starting point which locates in the plane. The direction vector is also normalized to reduce the parameters. Finally, the line parameters are reduced from six to four (Ayache and Faugeras, 1989). The parameters reduction can be referred to plane $X=0$, $Y=0$ or $Z=0$. The selection of reference planes is based on the angle between line segment and normal vector of plane. The smaller angle represents the better geometry. Hence, we can avoid the problem of no intersection point between line segment and reference when they are parallel. Equation 4 demonstrates the function when reference plane $Z=0$ is applied. Figure 3 shows the geometry of the line segment.

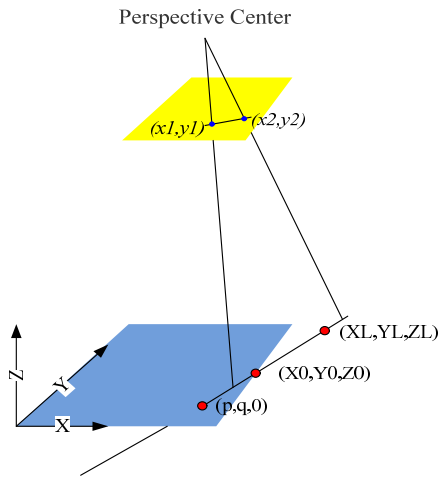


Figure 3. Representation of line-segment.

$$\begin{bmatrix} X_s \\ Y_s \\ Z_s \end{bmatrix} = \begin{bmatrix} X_0 \\ Y_0 \\ Z_0 \end{bmatrix} + t \begin{bmatrix} dX \\ dY \\ dZ \end{bmatrix} = \begin{bmatrix} p \\ q \\ 0 \end{bmatrix} + s \begin{bmatrix} a \\ b \\ 1 \end{bmatrix} \quad (4)$$

In Equation 4, (X_s, Y_s, Z_s) are the coordinates of a point located in a line; (X_0, Y_0, Z_0) are the starting point of a line; (dX, dY, dZ) are the direction vector; $(p, q, 0)$ are the starting point through the plane of $Z=0$; $(a, b, 1)$ are the normalized direction vector; t and s are the scale factor of a line.

We establish the line-based collinearity equations by combining Equations 1 and 4. The new equation is shown as Equation 5. Compared with the point-based collinearity equations, the additional unknowns for line-based equations are the scale factor of a line. We linearize the equations and solve the parameters iteratively. The matrix and the elements are shown in Equations 6 and 7.

$$\begin{aligned} x &= x_0 - f \frac{m_{11}(p + s*a - X^c) + m_{12}(q + s*b - Y^c) + m_{13}(s - Z^c)}{m_{31}(p + s*a - X^c) + m_{32}(q + s*b - Y^c) + m_{33}(s - Z^c)} \\ y &= y_0 - f \frac{m_{21}(p + s*a - X^c) + m_{22}(q + s*b - Y^c) + m_{23}(s - Z^c)}{m_{31}(p + s*a - X^c) + m_{32}(q + s*b - Y^c) + m_{33}(s - Z^c)} \end{aligned} \quad (5)$$

In Equation 5, (x, y) are the image coordinates; (x_0, y_0) are the principal points; (X, Y, Z) are the object coordinates; $(p, q, 0)$ and $(a, b, 1)$ are the parameters of control line; s is the scale factor of a line; $(m_{11} \sim m_{33})$ are the elements of rotation matrix from rotation angles (ω, ϕ, κ) ; f is the focal length.

$$V_l = \begin{bmatrix} B_{l1} & B_{l2} \end{bmatrix} \begin{bmatrix} \Delta_p \\ \Delta_l \end{bmatrix} - L_l \quad (6)$$

In Equation 6, V_l is the vector of residual errors; B_{l1} and B_{l2} are the matrix of the coefficients of unknowns; Δ_p is the vector of unknown corrections of exterior parameters; Δ_l is the vector of unknown corrections of scale factor; L_l is the vector of constant terms.

$$\begin{bmatrix} V_{y1} \\ \vdots \\ V_{yn} \\ V_{zn} \end{bmatrix} = \begin{bmatrix} \frac{\partial F_1^c}{\partial X^c} & \frac{\partial F_1^c}{\partial Y^c} & \frac{\partial F_1^c}{\partial Z^c} & \frac{\partial F_1^c}{\partial \omega} & \frac{\partial F_1^c}{\partial \phi} & \frac{\partial F_1^c}{\partial \kappa} & \frac{\partial F_1^c}{\partial s_1} & \vdots & 0 \\ \frac{\partial G_1^c}{\partial X^c} & \frac{\partial G_1^c}{\partial Y^c} & \frac{\partial G_1^c}{\partial Z^c} & \frac{\partial G_1^c}{\partial \omega} & \frac{\partial G_1^c}{\partial \phi} & \frac{\partial G_1^c}{\partial \kappa} & \frac{\partial G_1^c}{\partial s_1} & \vdots & 0 \\ \vdots & \vdots \\ \frac{\partial F_n^c}{\partial X^c} & \frac{\partial F_n^c}{\partial Y^c} & \frac{\partial F_n^c}{\partial Z^c} & \frac{\partial F_n^c}{\partial \omega} & \frac{\partial F_n^c}{\partial \phi} & \frac{\partial F_n^c}{\partial \kappa} & \frac{\partial F_n^c}{\partial s_n} & \vdots & \vdots \\ \frac{\partial G_n^c}{\partial X^c} & \frac{\partial G_n^c}{\partial Y^c} & \frac{\partial G_n^c}{\partial Z^c} & \frac{\partial G_n^c}{\partial \omega} & \frac{\partial G_n^c}{\partial \phi} & \frac{\partial G_n^c}{\partial \kappa} & \frac{\partial G_n^c}{\partial s_n} & \vdots & \vdots \end{bmatrix} \begin{bmatrix} \Delta X^c \\ \Delta Y^c \\ \Delta Z^c \\ \Delta \omega \\ \Delta \phi \\ \Delta \kappa \\ \Delta s_1 \\ \vdots \\ \Delta s_n \end{bmatrix} - \begin{bmatrix} F_1^c \\ G_1^c \\ \vdots \\ F_n^c \\ G_n^c \end{bmatrix} \quad (7)$$

2.3 Space Resection by Point and Line Features

In this section, we introduce space resection by integrating the point and linear features. Figure 4 shows the idea of space resection using point and linear features. There are some advantages of using both features in space resection. For example, when the point and linear features are both available, we can use the complete information to determine the exterior orientations simultaneously. Moreover, the controlling capability of control points is geometrically stronger than control line. If we add some control points with control line in space resection, it improves the accuracy of exterior orientations. We establish a joint model by combining Equations 2 and 6. The new equation is shown as Equation 8.

This joint adjustment model needs to linearize for least squares adjustment. A number of initial values are needed to obtain an approximate value. The initial values of exterior orientation parameters can be determined by Direct Linear Transformation (Kobayashi and Mori, 1997). The other initial value is the scale factor of a line segment which can be derived from two end points. Nowadays, GPS is mounted on specific camera for camera position. This information is useful for the initial values of a camera position.

$$\begin{bmatrix} V_p \\ V_l \end{bmatrix} = \begin{bmatrix} B_p & 0 \\ B_{l1} & B_{l2} \end{bmatrix} \begin{bmatrix} \Delta_p \\ \Delta_l \end{bmatrix} - \begin{bmatrix} L_p \\ L_l \end{bmatrix} \quad (8)$$

In Equation 8, V_p and V_l are the matrix of residual errors; B_p , B_{l1} and B_{l2} are the matrix of the coefficients of unknowns; Δ_p is the matrix of unknown corrections of exterior parameters; Δ_l is the matrix of unknown corrections of scale factor; L_p and L_l are the matrix of constant terms.

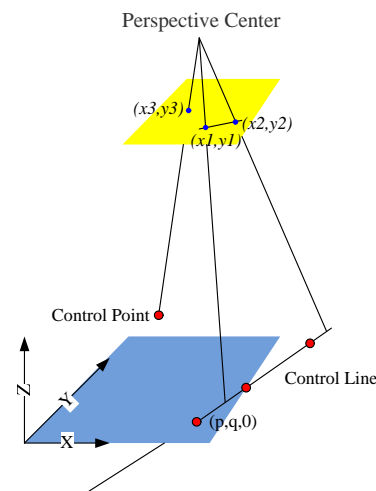


Figure 4. Space resection by the integration of control point and control line.

3. EXPERIMENTAL RESULTS

Three data sets are selected in the experiment. The first one is a simulation data. The second one is an aerial image. The third one is a close-range image.

3.1 Simulation Data

Simulation data is used to verify the procedure. We simulate an aerial image with vertical imaging. In this simulation, we add random errors to the control features. The random errors are 0.5 pixels in the image space and 0.5 meters in the object space. We simulate 38 control points (CP) and 41 control lines (CL) in this study. The 372 independent check points (ICP) are used to evaluate the accuracy of the exterior parameters. Figure 5 shows the distribution of simulation data. For point-based space resection, the root mean square errors (RMSE) of ICP are 0.62 and 0.88 pixels in two directions. For line-based space resection, though the number of control line is more than the number of control point, the RMSE of ICP is still 0.87 and 1.01 pixels in x and y directions. The result of line-based space resection is not as good as point-based space resection. We combine 3 control points and 41 control lines in our proposed method. The RMSE of ICP improves to 0.79 and 1.00 pixels. We also combine all the control points and control lines in space resection. The RMSE of ICP improves to 0.38 and 0.56 pixels. Tables 1 and 2 summarize the results of simulation data without and with random error.

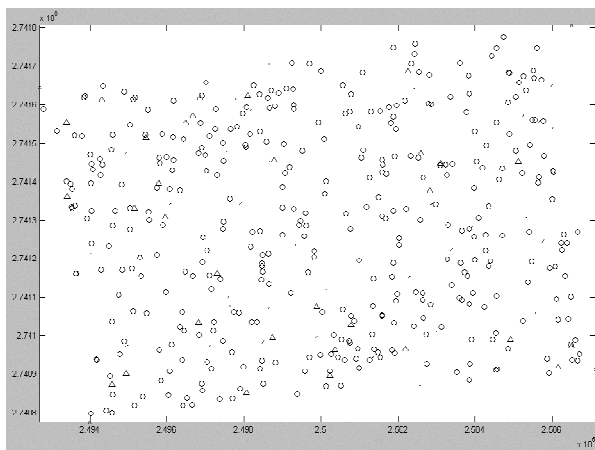


Figure 5. Distribution of control features of aerial image.

Table 6. Results of simulation data (without random error).

Unit: pixel	Point	Line	Point+Line
No. CP	38	0	38
No. CL	0	41	41
No. ICP	372	372	372
Mean Sample	-8.93E-06	-9.24E-06	-9.27E-06
Mean Line	3.12E-06	1.74E-06	1.84E-06
RMSE Sample	2.24E-04	2.26E-04	2.29E-04
RMSE Line	3.33E-04	3.34E-04	3.39E-04

Table 7. Results of simulation data (with random error).

Unit: pixel	Point	Line	Point+Line		
No. CP	38	0	1	3	38
No. CL	0	41	41	41	41
No. ICP	372	372	372	372	372
Mean Sample	0.44	0.44	0.41	0.27	0.03
Mean Line	0.68	0.08	0.06	-0.05	0.37
RMSE Sample	0.62	0.87	0.86	0.79	0.38
RMSE Line	0.88	1.01	1.00	1.00	0.56
$\sigma \omega$	0.0005	0.0005	0.0005	0.0005	0.0004
$\sigma \varphi$	0.0004	0.0005	0.0005	0.0005	0.0003
$\sigma \kappa$	0.0001	0.0001	0.0001	0.0001	0.0001
σX_c	0.5045	0.6916	0.6835	0.6815	0.3845
σY_c	0.6903	0.6939	0.6857	0.6809	0.4859
σZ_c	0.1596	0.1871	0.1842	0.1840	0.1142

3.2 Aerial Image

The second data is an aerial image with 3-D building models. The image was acquired by an UltraCamD with 1/12,000 image scale. The image size is 11500 x 7500 pixels. The ground resolution of the image is about 12cm. The accuracies of 3-D building corners are 20cm and 35cm in horizontal and vertical direction. We measure 10 control points and 10 control lines from the image and maps. The number of independent check points is 25. Figure 8 shows the distribution of control features superimposed with aerial image. The corresponding 3-D building models are shown as Figure 9. The geometric characteristics of aerial image are similar to simulation data. The RMSE of ICP is 1.87 and 2.26 pixels in x and y directions when we apply the point-based space resection. The RMSE of line-based space resection is 2.50 and 2.86 pixels. The RMSE of proposed method is 2.17 and 2.54 pixels. Table 10 summarizes the results of aerial image.



Figure 8. Distribution of control features of aerial image.

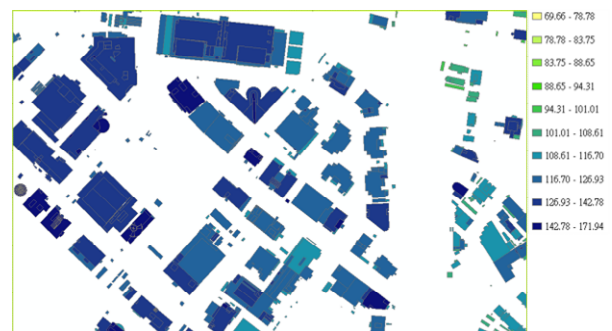


Figure 9. 3-D models for aerial image.

Table 10. Results of aerial image.

Unit: pixel	Point	Line	Point+Line		
No. CP	10	0	1	10	10
No. CL	0	10	10	1	10
No. ICP	25	25	25	25	25
Mean Sample	0.86	1.05	1.36	0.86	1.09
Mean Line	-0.92	-1.77	-1.67	-0.89	-1.35
RMSE Sample	1.87	2.49	2.46	1.87	2.17
RMSE Line	2.26	2.86	2.79	2.24	2.54

3.3 Close-range Image

For close-range image, the image scale is about 1/1,700. The resolution of the image is about 1cm. The image size is 4288 x 2848 pixels. The rough camera position is recorded by a GPS, which is mounted on the camera. The lens distortions are pre-calibrated by using commercial software, i.e., PhotoModeler. As the building detail in a building model is not very high, we can only measure a few control features. The accuracy of reference coordinates are 20cm and 35cm in horizontal and vertical direction.. The number of control points and lines are 4 and 7 respectively. We also measure 3 independent check points for accuracy evaluation. The distribution of control features are shown in Figure 11. The respective building models are shown in Figure 12. Notice that, the length of the control lines is quite long related to the image frame. For point-based space resection, the RMSE of ICP is 14.44 and 9.20 pixels in x and y directions. The RMSE of line-based space resection is 16.75 and 6.13 pixels. We also combine all the control points and control lines in space resection. The RMSE of ICP improves to 15.56 and 6.45 pixels. Table 10 summarizes the results of close-range image.



Figure 11. Distribution of control features of ground image.

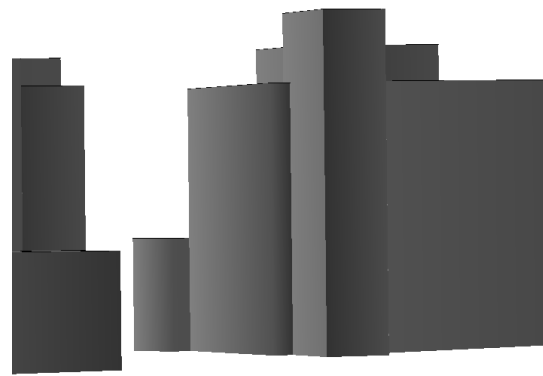


Figure 12. 3-D models for close-range image.

Table 13. Results of close-range image.

Unit: pixel	Point	Line	Point+Line
No. CP	4	0	4
No. CL	0	7	7
No. ICP	3	3	3
Mean Sample	5.82	9.53	7.76
Mean Line	0.42	-1.17	0.17
RMSE Sample	14.44	16.75	15.56
RMSE Line	9.20	6.13	6.45

4. CONCLUSIONS

In this research, we have proposed a feasible scheme to obtain the exterior orientations that integrates point and linear features. The simulation data show that the result of point-based adjustment is better than the line-based adjustment. The combine adjustment of these two features may improve the accuracy. If all the available data involve the adjustment, the best result is expected when compare to the other models. The accuracy of orientation for aerial image is around 2.5 pixels in this investigation. The resolution of image is 12cm and the accuracy of reference data is about 20cm to 35cm. For close-range image, the accuracy of orientations is better than 15 pixels. The resolution of image is 1cm. Hence, the accuracy in the object space is about 15cm. The results are based on the accuracy of 3-D building models. Thus, if the quality of model improves, the higher accuracy is expected.

REFERENCES

- Ayache, N., and Faugeras, O.D. 1989. *Maintaining representations of the environment of a mobile robot*, IEEE transactions on robotics and automation, 5(6), pp. 804-819.
- Akav, A., Zalmanson, G.H. and Doytsher, Y., 2004. *Linear feature based aerial triangulation*, *International Archives of Photogrammetry, Remote Sensing and Spatial Information Sciences*, pp. 7-12.
- Grussenmeyer, P. and Al Khalil, O., 2002. Solutions for exterior orientation in photogrammetry: a review. *Photogrammetric Record*, 17(100), pp. 615-634.

Habib, A., Ghanma, M., Morgan, M. and Al-Ruzouq, R., 2005. *Photogrammetric and lidar data registration using linear features*. *Photogrammetric Engineering and Remote Sensing*, 71(6), pp. 699-707.

Habib, A., Lin, H.T. and Morgan, M., 2003a. *Autonomous space resection using point- and line-based representation of free-form control linear features*. *Photogrammetric Record*, 18(103), pp. 244-258.

Jaw, J.J., 2000. *Control surface in aerial triangulation*, *International Archives of Photogrammetry, Remote Sensing and Spatial Information Sciences*, pp. 444-451.

Jaw, J.J. and Wu, Y.S., 2006. Control patches for automatic single photo orientation. *Photogrammetric Engineering And Remote Sensing*, 72(2), pp. 151-157.

Jung, F. and Boldo, d., 2004. *Bundle adjustment and incidence of linear features on the accuracy of external calibration parameters*, *International Archives of Photogrammetry, Remote Sensing and Spatial Information Sciences*, pp. 19-24.

Karjalainen, M., Hyypä, J. and Kuittinen, R., 2006. *Determination of exterior orientation using linear features from vector maps*. *Photogrammetric Record*, 21(116), pp. 329-341.

Kobayashi, K. and Mori, C., 1997. *Relations between the coefficients in the projective transformation equations and the orientation elements of a photograph*. *Photogrammetric Engineering & Remote Sensing*, 63(9), pp. 1121–1127.

Schenk, T., 2004. *From point-based to feature-based aerial triangulation*. *ISPRS Journal of Photogrammetry and Remote Sensing*, 58(5-6), pp. 315-329.

Wolf, P.R. and Dewitt, B.A., 2000. *Elements of Photogrammetry: With Applications in GIS*. McGraw-Hill, 608 pp.

Zitova, B. and Flusser, J., 2003. *Image registration methods: a survey*. *Image and Vision Computing*, 21(11), pp. 977-1000.

ACKNOWLEDGEMENTS

This investigation was partially supported by the National Science Council of Taiwan under project number NSC 98-2218-E-009 -018. The authors would like to thank the Chinese Society of Photogrammetry and Remote Sensing of Taiwan for providing the test data sets.